PHYSICAL REVIEW B **86**, 100505(R) (2012)

Emergence of superconductivity in $BaNi_2(Ge_{1-x}P_x)_2$ at a structural instability

Daigorou Hirai, F. von Rohr,* and R. J. Cava
Department of Chemistry, Princeton University, Princeton, New Jersey 08544, USA
(Received 14 July 2012; revised manuscript received 5 September 2012; published 19 September 2012)

The physical properties and structural evolution of the 122-type solid solution $BaNi_2(Ge_{1-x}P_x)_2$ are reported. The in-plane X-X ($X = Ge_{1-x}P_x$) dimer formation present in the end member $BaNi_2Ge_2$, which results in a structural transition to orthorhombic symmetry, is completely suppressed to zero temperature on P substitution near $x = 0.7$, and a dome-shaped superconducting phase with a maximum $T_c = 2.9$ K emerges. Clear indications of phonon softening and enhanced electron-phonon coupling are observed at the composition of the structural instability. Our findings show that dimer breaking offers possibilities as a tuning parameter of superconductivity.

DOI: 10.1103/PhysRevB.86.100505 PACS number(s): 74.70.Dd, 74.25.Dw, 61.50.Ks, 74.25.Bt

Several superconductors with high transition temperatures (T_c) are located near structural instabilities, for example, A15 compounds,[1] perovskite bismuthates,[2] cubic tungsten bronzes,[3] and intercalated graphite under high pressure.[4,5] The instability that leads to the structural phase transition is characterized by phonon softening, and the resulting enhanced electron-phonon coupling is believed to play a significant role for the high T_c's. The relationships between structural instabilities and superconductivity have provided much work of interest in the past 50 years.

The tetragonal $ThCr_2Si_2$ ("122") structure type is a layered structure with edge-sharing transition metal-metalloid TX_4 tetrahedra making T_2X_2 layers that alternate with layers of the large A atoms (A: alkali metal, alkaline earth metal, rare earth; T: transition metal; X: metalloid). Previous studies have revealed that some AT_2X_2 compounds are located at a structural instability between two different 122 structural types: a collapsed tetragonal (cT) phase and an uncollapsed tetragonal (ucT) phase.[6,7] The structural change from ucT to cT, resulting in significantly reduced ratios of stacking to in-plane lattice parameters (i.e., c/a) is driven by the formation of a moleculelike X-X dimer across the A atom layer. Lattice collapse transitions from the ucT to the cT phase can be controlled by applied physical[8–10] and chemical pressures,[11–13] and recent research has demonstrated the usability of chemical bond breaking as a tuning parameter to control physical properties.[14–16]

$BaNi_2P_2$ is a ucT 122-type superconductor with a T_c of 2.5 K.[17,18] $BaNi_2Ge_2$, on the other hand, is a 122-type normal metal with a lattice distortion due to Ge-Ge dimer formation, but not of the cT-ucT lattice collapse type. It crystallizes in an ordinary ucT $ThCr_2Si_2$-type structure at high temperature, but exhibits a structural transition to an orthorhombic phase (space group *Pnma*) on cooling below 753 K.[19] The important consequence of the structural transition is that equal Ge-Ge distances in the Ni_2Ge_2 layers at high temperature (3.61 Å at 783 K) are split into one short distance (2.93 Å at 753 K) and two much longer distances (3.69 and 3.72 Å at 753 K) below the phase transition, as shown in Fig. 1(a). This structural transition is the result of in-plane Ge-Ge dimer formation in the Ni_2Ge_2 layer. This unusual structural instability is driven by the strong tendency toward Ge-Ge bonding in 122-type structures as a consequence of the electron count[6] even though, due to the presence of the large Ba ion, the layers are too far apart in $BaNi_2Ge_2$ for the usual X-X bond across the A layer seen in the cT phases.

In this Rapid Communication, we demonstrate the systematic suppression of the in-plane dimer phase of $BaNi_2Ge_2$ by P doping. A dome-shaped superconducting phase emerges at the structural instability where the dimer phase is suppressed and a ucT phase appears. The enhanced specific-heat jump at the superconducting transition at the critical border of instability of the dimer phase and the ucT phase strongly suggests that phonon softening induced by dimer breaking is responsible for the enhanced T_c. Our finding demonstrates that dimer breaking offers a possibility as a tuning parameter of superconductivity.

Conventional solid-state reactions were employed to synthesize the polycrystalline samples. As the first step, $BaNi_2P_2$ and $BaNi_2Ge_2$ were made by mixing elemental Ba (99%), Ni (99.9%), and P (red, 99%) or Ge (99.9999%) at a ratio of 1.05:2:2 in an argon filled glove box. The mixed powder was placed in an alumina crucible and sealed in an evacuated quartz tube, and then sintered initially at 550 °C for 10 h and 800 °C for 48 h. Then, $BaNi_2P_2$ and $BaNi_2Ge_2$ were mixed as $BaNi_2(Ge_{1-x}P_x)_2$ for $0 < x < 1$, heated at 800 °C for 24 h. The sintered pellet was reground, repelletized, and sintered again at 800 °C for 24 h.

All products were initially characterized by laboratory powder x-ray diffraction (XRD, Bruker D8, Cu $K\alpha$ radiation). Selected samples were characterized with high resolution synchrotron powder diffraction at beamline 11-BM at the Advanced Photon Source (APS) at Argonne National Laboratory using an average wavelength of 0.413 08 Å. The structures were refined by the Rietveld method using the FULLPROF program.[20]

Magnetic susceptibility, resistivity, and heat capacity measurements were performed by a magnetic properties measurement system (MPMS: Quantum Design) and a physical property measurement system (PPMS: Quantum Design). Specific-heat measurements down to 0.4 K were performed in a PPMS equipped with a ^{3}He insert.

The structural instability that results from in-plane dimer breaking, which can be recognized as the structural transition from an orthorhombic phase to a tetragonal phase, was clearly observed between $x = 0.2$ and 0.4 in the room-temperature XRD patterns. As shown in the inset of Fig. 1, the 112 and 011 peaks in the orthorhombic cell at low P content become a single 112 peak in the tetragonal cell above a P content of

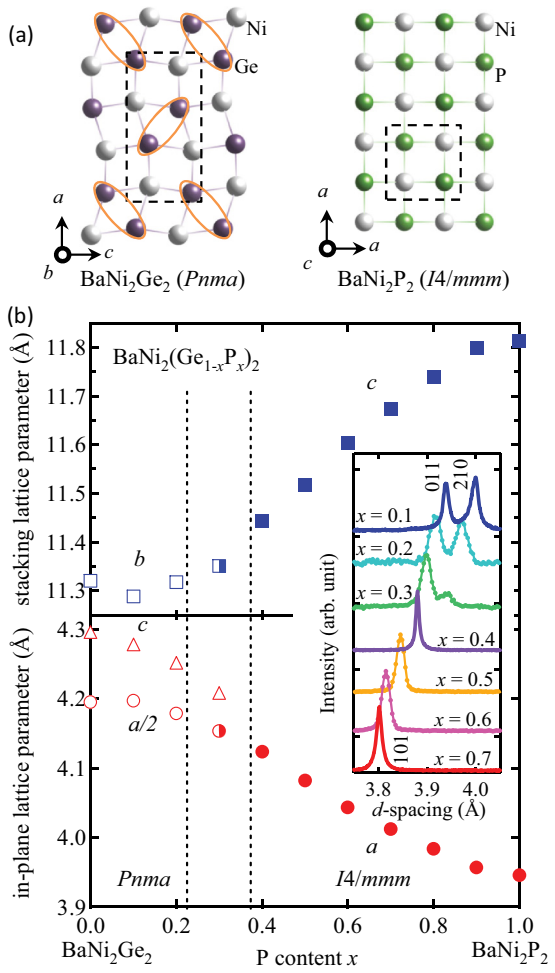

FIG. 1. (Color online) (a) A comparison of the P and Ge atom planes in the crystal structures of $BaNi_2P_2$ ($I4/mmm$) and $BaNi_2Ge_2$ ($Pnma$). Dotted squares represent unit cells. The ovals indicate the shortest Ge-Ge bonds in the Ni_2Ge_2 layer. (b) The P content dependence of the in-plane and perpendicular-to-plane lattice parameters of $BaNi_2(Ge_{1-x}P_x)_2$. The inset is an enlarged XRD pattern showing the change in the crystal symmetry with P content. Bold lines and dots represent synchrotron and laboratory XRD patterns, respectively.

$x = 0.3$. This disappearance of peak splitting indicates that the distortion of the Ni_2X_2 ($X = Ge_{1-x}P_x$) layers originating from the X-X dimer formation is relaxed and that the Ni_2X_2 lattice becomes a regular square.

The XRD pattern for $x = 0.3$ can be refined with a mixture of tetragonal $BaNi_2P_2$-like and orthorhombic $BaNi_2Ge_2$-like phases with a ratio of 6:4. There is no indication of chemical phase separation into $BaNi_2P_2$-like and $BaNi_2Ge_2$-like phases, except for $x = 0.3$, in $BaNi_2(Ge_{1-x}P_x)_2$, and the XRD patterns of $BaNi_2(Ge_{1-x}P_x)_2$ with x below and above 0.3 were well refined with orthorhombic ($Pnma$) and tetragonal cells ($I4/mmm$), respectively. The systematic change in the room-temperature XRD pattern indicates that the dimer formation at 753 K in $BaNi_2Ge_2$ (Ref. 19) is driven down in temperature by P substitution and straddles room temperature at a P content of $x = 0.3$.

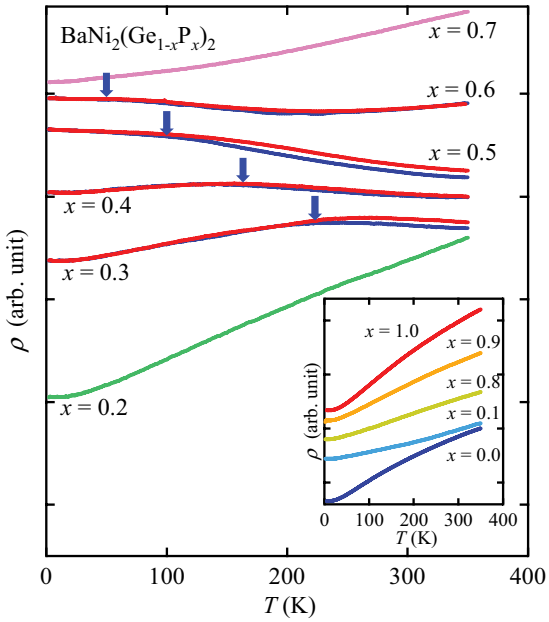

FIG. 2. (Color online) The temperature dependence of the electrical resistivity of $BaNi_2(Ge_{1-x}P_x)_2$ with various P concentrations. Each data set is normalized by the resistivity value at 350 K and shifted to avoid overlap. Arrows indicate the low-temperature end points of the hysteresis.

Figure 1 shows the room-temperature lattice parameters as a function of P concentration for $BaNi_2(Ge_{1-x}P_x)_2$ determined by the refinement of the XRD data. The b axis (c axis in the tetragonal phase), a measure of unit cell perpendicular to the Ni_2X_2 layers, decreases monotonically, but nonlinearly, with P content x. On the other hand, the a and c axes (a axis in the tetragonal phase), measures of the Ni_2X_2 in-plane dimensions, increase. This anisotropic change in lattice parameters with increasing P content is in striking contrast to what is seen in the highly analogous conventional solid solution $LaNi_2(Ge_{1-x}P_x)_2$, where they decrease monotonically with increasing P content[21] due to the simple chemical pressure effect that occurs when substituting P (atomic radius of 1.00 Å) for Ge (atomic radius of 1.25 Å).[22] When the Ge is totally substituted by P, the crystal structure of $BaNi_2P_2$ is in a ucT phase with a large ratio of stacking to in-plane lattice parameters (c/a) of 3.0, consistent with previous reports.[23]

As the transition temperature of in-plane dimer breaking (T_s) is suppressed with increasing P content, T_s comes into the temperature range of our resistivity measurements and is clearly observed above $x = 0.3$, as shown in Fig. 2. All the $BaNi_2(Ge_{1-x}P_x)_2$ samples have resistivities below 1 mΩ cm at 300 K, indicating the metallic nature of these compounds. The resistivities of both of the end members $BaNi_2Ge_2$ ($x = 0$) and $BaNi_2P_2$ ($x = 1$) show a monotonic decrease on cooling without any anomaly. In the intermediate doping range of $x =$ 0.3–0.6, however, the resistivity data show a local maximum accompanied by hysteresis. The clear hysteresis in resistivity data indicates that the dimer breaking transition is of first order. From $x = 0.3$ to 0.6 the peak position systematically decreases in temperature and the hysteresis smears out. Finally, the anomaly completely disappears above a P content of $x = 0.7$ and normal metallic behavior is recovered.

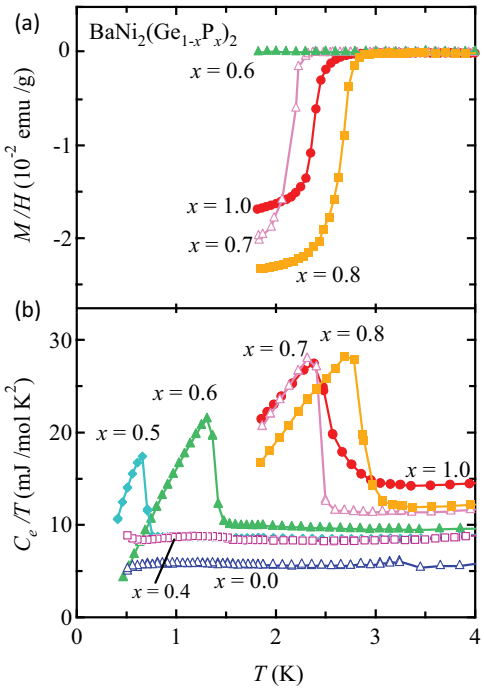

FIG. 3. (Color online) The temperature dependence of the dc magnetization (M/H) under an applied magnetic field of 10 Oe and the electronic part of the specific heat divided by temperature (C_e/T) for $BaNi_2(Ge_{1-x}P_x)_2$.

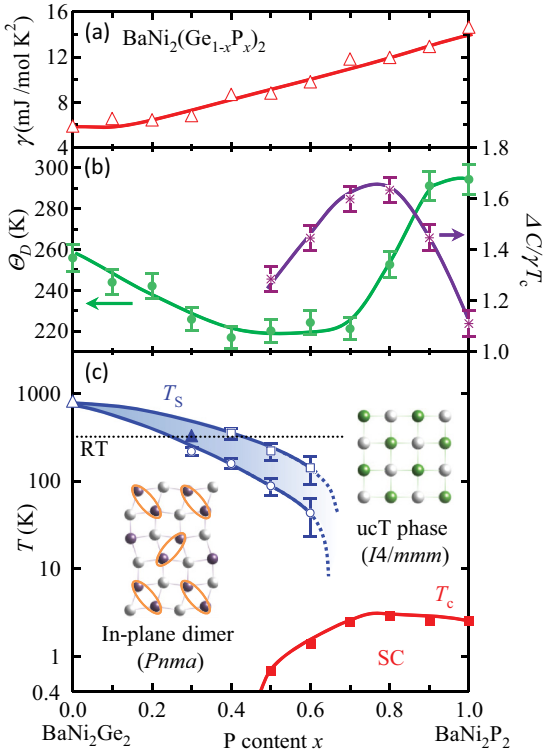

FIG. 4. (Color online) The P content dependence of (a) The electronic specific-heat coefficients (γ). (b) The Debye temperatures (Θ_D) obtained from low-temperature fits of the specific-heat data and the normalized specific-heat jumps at T_c ($\Delta C/\gamma T_c$). Error bars for γ are less than the point size. (c) The electronic phase diagram (logarithmic T) of $BaNi_2(Ge_{1-x}P_x)_2$. Solid squares represent superconducting transition temperatures (T_c) determined from heat capacity measurements. Solid and open triangles are the structural transition temperatures (T_s) determined by powder XRD data and obtained from Ref. 10, respectively. Open squares and circles represent, respectively, the T_s upon cooling and heating determined from the resistivity data.

When the structural transition observed through the anomaly in the resistivity data of $BaNi_2(Ge_{1-x}P_x)_2$ is completely suppressed at a P content $x = 0.7$, a superconducting transition is observed in low-temperature magnetization data. Figure 3(a) shows that a large diamagnetic signal hallmarking bulk superconductivity is observed in the samples with a P content of $x = 0.7$–1.0. The T_c reaches a maximum of about 2.9 K for $x = 0.8$ and then decreases slightly for higher P content. The $T_c = 2.5$ K for the $x = 1$ compound $BaNi_2P_2$ is consistent with the previous report for a single crystal.[18] Further investigation of the superconducting phase down to 0.4 K was performed by a heat capacity measurement. A large heat capacity jump corresponding to the superconducting transition is clearly observed in $BaNi_2(Ge_{1-x}P_x)_2$ with $x \geqslant 0.7$ [Fig. 3(b)]. Superconducting transitions were also observed for the lower P contents of $x = 0.4$–0.6. Below $x = 0.3$, superconductivity is no longer observed above our lowest measurement temperature of 0.4 K. All the samples show very sharp transitions, indicating that they are highly homogeneous.

A detailed analysis of the low-temperature specific-heat data shows clear indication of the criticality of the dimer-breaking structural instability. The normal-state heat capacity data under an applied field that suppresses the superconductivity can be well fitted by the equation $C/T = \gamma + \beta T^2$, where γ is the electronic specific-heat coefficient and β is the phonon contribution. As the P content increases, γ increases monotonically from $BaNi_2Ge_2$ to $BaNi_2P_2$, while the Debye temperature (Θ_D) calculated from β has a minimum around the structural phase instability, as shown in Figs. 4(a) and 4(b). A similar suppression of Θ_D and the emergence of superconductivity have been reported in Pd- and Pt-doped $IrTe_2$ at the critical concentration where the structural transition characterized by Ir-Ir bond formation is completely suppressed.[24,25] In contrast, both γ and β of $LaNi_2(Ge_{1-x}P_x)_2$, where the end members $LaNi_2Ge_2$ and $LaNi_2P_2$ crystallize in the same cT structure type, decrease monotonically with increasing P content.[21]

The criticality can be more clearly observed in the normalized specific-heat jump at the superconducting transition ($\Delta C/\gamma T_c$), as shown in Fig. 4(b). The value of $\Delta C/\gamma T_c$ exhibits a clear maximum centered at the composition boundary between the dimer and ucT phases. The Fermi surface and transport properties of the $BaNi_2P_2$ superconductor are distinct from those of the iron-pnictide superconductors[18,26] and $BaNi_2P_2$ is considered to be a phonon-mediated conventional superconductor. Considering that $\Delta C/\gamma T_c$ can be underestimated due to nonsuperconducting contributions to γ and the broadness of the superconducting transition, the value of $\Delta C/\gamma T_c \sim 1.1$ for $BaNi_2P_2$ agrees reasonably with a BCS weak coupling value of 1.43. At $x = 0.8$, however, $\Delta C/\gamma T_c$ increases by 50%, reaching 1.63 and suggesting strong electron-phonon coupling.

As summarized in the electronic phase diagram [Fig. 4(c)], the emergence of the superconducting phase in $BaNi_2(Ge_{1-x}P_x)_2$ is strongly correlated with the structural instability caused by the in-plane dimer breaking transition. When the P content x increases, the room-temperature crystal structure changes from orthorhombic to tetragonal at $x = 0.3$, and the anomaly in resistivity data, indicative of the structural phase transition, is driven down in temperature. A superconducting phase emerges at $x = 0.5$, and T_c abruptly increases with the dimer phase suppressed; finally T_c reaches a maximum at $x = 0.8$ when the dimer is fully broken.

Electronic-structure calculations show that the valence band around the Fermi level in $BaNi_2P_2$ is formed predominantly by a strongly hybridized transition-metal d and metalloid p states.[27] With the presence of covalent Ge-Ge in-plane bonding, the Fermi level for $BaNi_2Ge_2$ must be located between the bonding orbitals (σ) and antibonding orbitals (σ^*) of the Ge-Ge dimer. The dimer is absent in $BaNi_2P_2$ due to the higher electron count, which results in occupancy of the antibonding σ^* dimer band. Therefore, the structural instability in $BaNi_2(Ge_{1-x}P_x)_2$ is brought about by doping electrons into the X-X dimer antibonding orbital.[6] This complements our recent research on $SrCo_2(Ge_{1-x}P_x)_2$ (Ref. 11) and $LaCo_2(Ge_{1-x}P_x)_2$,[13] which revealed that a conventional lattice collapse transition, a result of interlayer X-X dimer formation, can be controlled by P doping of germanides. Hall coefficient measurements (not shown) indicate that P substitution does not simply dope $BaNi_2(Ge_{1-x}P_x)_2$ with electrons, consistent with electronic-structure calculations on this phase[27] that predicted to have a multiband character at Fermi energy.

In contrast to the gradual increase in γ, clear criticality is observed in both the Debye temperatures and specific-heat jumps at T_c in the $BaNi_2(Ge_{1-x}P_x)_2$ system. These observations lead us to propose that enhanced electron-phonon coupling due to softening phonons is responsible for the enhancement of T_c at the boundary of the dimer breaking structural instability. An enhancement of T_c at the boundary of two different structures has been reported, for example, in tellurium under high pressure, where T_c jumps from 2.5 to 7.4 K.[28] First-principles calculations have pointed out that the jump in T_c in that case can be explained by the enhancement of the electron-phonon interaction.[29] Recently, Kudo *et al.* found a discontinuous increase in T_c from 0.6 to 3.3 K in $BaNi_2(As_{1-x}P_x)_2$ at the boundary of a triclinic lower P content phase and a tetragonal high P content phase.[30] A similar reduction in Debye temperature and enhanced $\Delta C/\gamma T_c$ is observed in that system. It is interesting to note that T_c shows a stepwise increase in both Te and $BaNi_2(As_{1-x}P_x)_2$ at the phase boundary, in contrast to the dome-shaped superconducting phase in $BaNi_2(Ge_{1-x}P_x)_2$. Further theoretical and experimental investigations, especially on soft phonon modes in 122 structure types, will be useful to clarify the difference between these systems and to look at the possibilities for achieving superconductivity with higher T_c's. The strong correlation between the structural transition and superconductivity $BaNi_2(Ge_{1-x}P_x)_2$ gives rise to an opportunity for employing dimer breaking as a control parameter of superconductivity.

The authors thank B. Toby, L. Ribaud, and M. Suchomel at beamline 11-BM at the APS for their excellent diffraction data, and L. M. Schoop for helpful discussions. This work was supported by the US DOE Office of Basic Energy Sciences, Grant No. DE-FG02-45706. Use of the APS at Argonne National Laboratory was supported by the US DOE, Office of Science, Office of Basic Energy Sciences, under Contract No. DE-AC02-06CH11357.

*Present address: Physik-Institut, Universität Zürich, Winterthurerstrasse 190, CH-8057 Zürich, Switzerland.

[1] L. R. Testardi, Rev. Mod. Phys. **47**, 637 (1975).
[2] D. G. Hinks, D. R. Richards, B. Dabrowski, D. T. Marx, and A. W. Mitchell, Nature (London) **335**, 419 (1988).
[3] H. R. Shanks, Solid State Commun. **15**, 753 (1974).
[4] J. S. Kim, L. Boeri, R. K. Kremer, and F. S. Razavi, Phys. Rev. B **74**, 214513 (2006).
[5] A. Gauzzi, S. Takashima, N. Takeshita, C. Terakura, H. Takagi, N. Emery, C. Herold, P. Lagrange, and G. Loupias, Phys. Rev. Lett. **98**, 067002 (2007).
[6] R. Hoffman and C. Zheng, J. Phys. Chem. **89**, 4175 (1985).
[7] G. Just and P. Paufler, J. Alloys Compd. **232**, 1 (1996).
[8] P. Canfield, S. Bud'ko, N. Ni, A. Kreyssig, A. Goldman, R. McQueeney, M. Torikachvili, D. Argyriou, G. Luke, and W. Yu, Physica C **469**, 404 (2009).
[9] C. Huhnt, W. Schlabitz, A. Wurth, A. Mewis, and M. Reehuis, Phys. Rev. B **56**, 13796 (1997).
[10] M. Chefki, M. M. Abd-Elmeguid, H. Micklitz, C. Huhnt, W. Schlabitz, M. Reehuis, and W. Jeitschko, Phys. Rev. Lett. **80**, 802 (1998).
[11] S. Jia, A. J. Williams, P. W. Stephens, and R. J. Cava, Phys. Rev. B **80**, 165107 (2009).
[12] S. Jia, S. Chi, J. W. Lynn, and R. J. Cava, Phys. Rev. B **81**, 214446 (2010).
[13] S. Jia and R. J. Cava, Phys. Rev. B **82**, 180410(R) (2010).
[14] S. Jia, P. Jiramongkolchai, M. R. Suchomel, B. H. Toby, J. G. Checkelsky, N. P. Ong, and R. J. Cava, Nat. Phys. **7**, 207 (2011).
[15] K. Kovnir, W. M. Reiff, A. P. Menushenkov, A. A. Yaroslavtsev, R. V. Chernikov, and M. Shatruk, Chem. Mater. **23**, 3021 (2011).
[16] K. Kovnir, V. O. Garlea, C. M. Thompson, H. D. Zhou, W. M. Reiff, A. Ozarowski, and M. Shatruk, Inorg. Chem. **50**, 10274 (2011).
[17] T. Mine, H. Yanagi, T. Kamiya, Y. Kamihara, M. Hirano, and H. Hosono, Solid State Commun. **147**, 111 (2008).
[18] Y. Tomioka, S. Ishida, M. Nakajima, T. Ito, H. Kito, A. Iyo, H. Eisaki, and S. Uchida, Phys. Rev. B **79**, 132506 (2009).
[19] V. Hlukhyy, A. Senyshyn, D. Trots, and T. F. Fässler, HASYLAB Annual Report 2007 (HASYLAB, Hamburg, 2007), Part 1, p. 1021.
[20] J. Rodriguez-Carvajal, Physica B **192**, 55 (1993).
[21] R. J. Goetsch, V. K. Anand, A. Pandey, and D. C. Johnston, Phys. Rev. B **85**, 054517 (2012).
[22] J. C. Slater, J. Chem. Phys. **41**, 3199 (1964).
[23] V. Keimes, D. Johrendt, A. Mewis, C. Huhnt, and W. Schlabitz, Anorg. Allg. Chem. **23**, 1699 (1997).
[24] J. J. Yang, Y. J. Choi, Y. S. Oh, A. Hogan, Y. Horibe, K. Kim, B. I. Min, and S-W. Cheong, Phys. Rev. Lett. **108**, 116402 (2012).

[25]S. Pyon, K. Kudo, and M. Nohara, J. Phys. Soc. Jpn. **81**, 053701 (2012).

[26]T. Terashima, M. Kimata, H. Satsukawa, A. Harada, K. Hazama, M. Imai, S. Uji, H. Kito, A. Iyo, H. Eisaki, and H. Harima, J. Phys. Soc. Jpn. **78**, 033706 (2009).

[27]I. R. Shein and A. L. Ivanovskii, Phys. Rev. B **79**, 054510 (2009).

[28]Y. Akahama, M. Kobayashi, and H. Kawamura, Solid State Commun. **84**, 803 (1992).

[29]F. Mauri, O. Zakharov, S. de Gironcoli, S. G. Louie, and M. L. Cohen, Phys. Rev. Lett. **77**, 1151 (1996).

[30]K. Kudo, M. Takasuga, Y. Okamoto, Z. Hiroi, and M. Nohara, Phys. Rev. Lett. **109**, 097002 (2012).